

Morphological and Molecular Identification of *Passalurus Ambiguus* Rudolphi, 1819 in Domestic Rabbits (*Oryctolagus Cuniculus*) in Qena Governorate, Upper Egypt

Nermean Moamen Hussein (✉ nermeanmohu@yahoo.com)

South Valley University <https://orcid.org/0000-0002-6003-5710>

Soheir A. H. Rabie

South Valley University Faculty of Science

Wafaa A. Abuelwafa

South Valley University Faculty of Science

Mouchira M. Mohi ELDin

South Valley University Faculty of Veterinary Medicine

Research Article

Keywords: Domestic rabbits, *Passalurus ambiguus*, Light and scanning electron microscopy, Histopathology, Phylogeny, Appendix, Egypt

Posted Date: November 30th, 2021

DOI: <https://doi.org/10.21203/rs.3.rs-1101490/v1>

License: © ⓘ This work is licensed under a Creative Commons Attribution 4.0 International License. [Read Full License](#)

Abstract

Domestic rabbits in Egypt are used commercially for meat, but gastrointestinal disorders can affect production. *Passalurus ambiguus* is an intestinal parasite that infects the rabbit causing intestinal problems and death in severe cases. The present study collected domestic rabbits from several locations throughout the Qena Governorate in Upper Egypt. *Passalurus ambiguus* worms were detected in 90 out of 200 rabbits (45%). They were described morphologically using light and scanning electron microscopy. Males measured 4.622 mm (2.838–7.172 mm) in length and 0.278 mm (0.139–0.558 mm) in width. Females measured 5.622 mm (2.347–9.532 mm) in length, 0.314 mm, and (0.185–0.381 mm) in width. Phylogenetic results confirmed the identification of the worms as *Passalurus ambiguus*. They appeared as small white nodules in the appendix of the rabbits examined. Histopathologically, a heavy worm burden was observed inside the appendiceal lumen, among crypts, and inside the lymphoid follicles. The heavy worm infestation leads to hyperplasia in the epithelial lining of the appendix and the follicles resulting in lumen obstruction. Granulomatous reactions were induced due to irritation and injury by the worm. It could be concluded that morphological features, molecular phylogenetic data, and histopathological findings clearly identified the present species as *Passalurus ambiguus* Rudolphi, 1819.

Introduction

The oxyurid *Passalurus ambiguus* can be found in the large intestine of both domestic and wild rabbits (Owen, 1972; Taffs, 1976). Moreover, it is the species with the best chances of adaptation to enteric culture farms (Grice and Prociv, 1993). *Passalurus ambiguus* infection of rabbits is not generally highly contagious. However, many pinworms are found in rabbits, and massive, fatal infections have been recorded in young rabbits (Owen, 1972). The parasite identification based on morphological characters is not fully reliable, leading to their misclassification. Therefore, it is important to expand the study area using PCR techniques to distinguish between different parasitic species.

Molecular methods have lately been employed to identify morphologically similar taxa, and they have greatly aided taxonomic, phylogenetic, and epidemiological research on several organisms (Yang et al., 2013; Ogedengbe et al., 2014; Li et al., 2015). These methods also provide excellent genetic markers for genetic variation in oxyurids, especially *Passalurus ambiguus* (Sheng et al., 2015; Abdel-Gaber et al., 2019; Solórzano-Garca et al., 2020). The goal of this work is to characterize the morphology of *Passalurus ambiguus*, which infects domestic rabbits in the Qena Governorate of Upper Egypt, in order to corroborate the molecular phylogenetic links between this species and other Oxyuroid species. Furthermore, the histopathological consequences of this species in the appendix of the rabbits studied were the focus of this research.

Materials And Methods

Sample collection

Ethics approval. The institutional ethics committee. Animal experiments followed the institutional ethical guidelines for the care and use of animals in research to the letter. Approval for animal studies were obtained from the Faculty of Veterinary medicine, South Valley University, Qena, Egypt (Approval number:25/13/11.2021).

200 domestic rabbits (*Oryctolagus cuniculus*) were collected at various locations and markets in Qena Governorate, Upper Egypt, from October 2018 to October 2020. Rabbits were transported to the Parasitology Laboratory, Department of Zoology, Faculty of Science, South Valley University, Qena.

Morphological analysis

A- Light microscopy

The gastrointestinal tract (GIT) was isolated and dissected, and the contents of the intestines were cleaned and sieved to eliminate the smallest particulates. As detailed by Georgi and Georgi (1990), nematodes were gathered using a stereomicroscope by screening diluted parts of intestinal material.

The recovered worms were fixed in a mixture of 70% ethanol and 5% glycerine and subsequently mounted on a slide with drops of lactophenol then covered by a coverslip (Meyer and Olsen, 1975). Some worms were stained with acetic alum carmine, dehydrated in ascending grades of ethanol alcohol (70 %, 80 %, 90%, 95%, and 100%), then cleared in xylene and mounted in DPX. The detected worms were identified according to (Danheim and Ackert, 1929; Skinner, 1931; Hugot et al., 1983; Petter and Quentin, 2009; Sultan et al., 2015; Abdel-Gaber et al., 2019; Mykhailiutenko et al., 2019).

B- Scanning electron microscopy

Specimens were submerged in a solution of 3 percent glutaraldehyde buffered with 0.1 M phosphate buffer (pH 4) for 2-4 hours at room temperature. Tissues were washed three times in 0.1 M phosphate buffer (pH 7.2) for ten minutes each time. Specimens were postfixed in a light

container for 2-4 hours at room temperature with 1-2 percent osmium tetroxide in 0.1 M phosphate buffer (pH 7.2). In graded ethanol/acetone solutions, dehydration occurs. Dehydration was done twice with 100% ethanol or acetone (15-30 minutes for each) (Hussein et al. 2018). Finally, worms were examined in the Central Laboratory of South Valley University using Jeol JSM-5500 LV Scanning electron microscope (Jeol, Japan) with a 20 KV accelerating voltage.

Molecular analysis

A. DNA extraction and sequencing

Specimens were removed from ethanol then distilled water was added to samples to completely remove the excess ethanol. The samples were placed individually in separate 1.5 ml microcentrifuge tubes, and DNA was extracted using genomic DNA mini kit (Quick- DNATM Funga/Bacterial Miniprep Kit).

PCR primers C1': ACCCGCTGAATTTAAGCAT and D2: TCCGTGTTTCAAGACGG were used to amplify the D1 and D2 domains of 28S rDNA from whole DNA (de Bellocq et al., 2001). PCR was carried out in a 25µl COSMO PCR RED Master Mix containing 1 µl template, 1 µM of each primer and Nuclease-free water to 50 µl. The following reaction conditions were used: (2 min initial denaturation at 95°C, then 25–35 cycles of 15 seconds at 95°C, 20 seconds at 50°C, and 30 seconds at 72°C. At 72°C, Post-PCR extension was performed for 1 minute). PCR products were examined on 2% agarose gels, stained with ethidium bromide, and photographed under a UV illuminator.

PCR amplification was purified using a DNA purification kit and subjected to automated DNA sequencing (ABI 3730XL DNA Sequencer, GATC Biotech, Germany) using the same primers used for PCR amplification.

B. Sequences of nematodes (partial 28S rDNA) from GenBank

The present study collected sequences from a partial 28S rDNA region for some related oxyuroid nematodes from GenBank. 13 partial 28S rDNA sequences from nematodes of the Superfamily Oxyuroidea (including outgroup from the Family Ascaridiidae) were obtained from the GenBank. These sequences were compared to the sequence collected in this study (Table 1).

C. Analysis of DNA sequences

The 13 partial 28S rDNA sequences from nematodes were edited with GeneStudio™ Professional Edition (version 2.2.0.0) and aligned with MEGA software (version 10.0.5) using default parameters.

D. Phylogenetic trees construction

On the basis of aligned partial 28S rDNA sequences, Oxyuroid nematode relationships were established using Maximum Likelihood (ML) and Maximum Parsimony (MP) approaches.

The ML and MP trees were obtained from the MEGA software (version 10.0.5). For ML analyses, the selected best-fit model and parameters by Hasegawa-Kishino-Yano model with five rate categories among sites (a discrete Gamma distribution [+G]) were used to construct an ML relationship tree. Bootstrap procedures were conducted with 1000 replications.

Histopathological analysis

Tissue specimens from the appendix were collected and fixed in 10% buffered formalin. After proper fixation, tissue blocks were embedded in paraffin. Thin (5 microns) sections were routinely prepared and stained with hematoxylin and eosin for the histopathological studies as described by (El-Akabawy et al., 2004).

Results

Taxonomic summary

Species: *Passalurus ambiguus* Rudolphi, 1819 (F: Oxyuridae)

Host: Domestic rabbits *Oryctolagus cuniculus* (F: Leporidae).

Locality: Qena Governorate, Upper Egypt.

Site of infection: Large intestine.

Prevalence: 45% (90 out of 200).

Intensity: 15–20 specimens of adult nematodes per infected rabbit.

A- Morphological analysis

The present study revealed the occurrence of *Passalurus ambiguus* that were seen by naked eye in the appendix and rectum of domestic rabbits (fig. 1 A). The enlarged appendix showing small white nodules (fig. 1 B). Worms attached in fecal pellets (fig. 1 C).

1- Light microscopy

Male (Based on 12 adult worms)

The length of the body is 4.622 mm (2.838–7.172 mm), the width is 0.278 mm (0.139–0.558 mm). The club-shaped esophagus measures 0.710 mm (0.391–0.1238 mm) in length (Figs. 2A, 3A, and 3C), the corpus measures 0.538 mm (0.274–0.908 mm) in length (Figs. 2B, 2C, 3B, 6A, and 6B), and the subspherical bulb measures 0.165 mm (0.094–0.304 mm) in diameter (Figs. 2B, 3B, and 6A). Testis (3A, 3C, and 6A) opens into thin-walled vas deferens. Vas deferens opens into the cloaca containing a single short protruded spicule measuring 0.094 mm (0.068–0.153 mm) in length (Figs. 2A, 2D, 2E, 3A, 3D, 6A, and 6C).

The cloaca was shown anteriorly by two pairs of large papillae (Figs. 2D, 2E, and 6C) and posteriorly by one pair of small papillae (Figs. 2D, 2E, 3D, and 6C). Two caudal papillae (Figs. 2D, 3C, and 6C) are present in the region of the tail. The body ended with a small coiled tail and measured 0.298 mm (0.145–0.492 mm) long (Figs. 2A, 2D, 3A, 3C, 6A, and 6C, and table 2).

Female (Based on 12 adult worms)

The body length is 5.622 mm (2.347–9.532 mm), and the width is 0.314 mm (0.185–0.381 mm). The club-shaped esophagus measures 0.484 mm (0.435–0.571 mm) in length (Figs. 4A and 5A), the corpus measures 0.369 mm (0.325–0.451 mm) in length (Figs. 4B, 4C, 5B, 6B, and 6D), and the subspherical bulb measures 0.124 mm (0.100–0.146 mm) in diameter (Figs. 4C, 5B, and 6D). Two large thin-walled ovaries (Figs. 5A and 6D) lie near the body wall and open posteriorly into the much-convoluted oviducts (Fig. 6D) packed with eggs in mature females. Eggs were elliptical with one side flattened, containing a knob in the anterior end, double thin walled and a developing embryo, and measuring 0.080 mm (0.075–0.088 mm) in length, and 0.034 mm (0.034–0.035 mm) in width (Figs. 4A, 4D, 5D, and 6F).

Oviducts empty into the straight transparent uterus (Fig. 6D) with its characteristically pointed end. The uterus continues as a straight tube with the vagina (Fig. 6D), which opens at the genital opening (Fig. 6D). Parallel to the uterus is a long tubule that connects to the vagina and extends posteriorly, ending in a convoluted mass in the anus region. From its position and structure, this tubule appears to be a rudimentary uterus and oviduct. The tail exhibits fine striations over the entire length, even showing through the annular bands and measuring 0.828 mm (0.579–0.945 mm) in length (Figs. 4A, 5A, 5C, 6D, and 6E, and table 2).

2- Scanning electron microscopy

In both males and females, transverse cuticular striations were visible on the body. Four papillae were found on the dorsal and ventral surfaces of *P. ambiguus*, indicating its anterior termination. The mouth was triangular and surrounded by three teeth (Figs. 7B, 8A, and 8B). No lips were seen.

Males of *Passalurus ambiguus* with a coiled posterior end, one short spicule (Figs. 7A, 7C, 7D, and 7E) protruding from the body in the cloacal region, and two pairs of large papillae around the cloaca, the second pair usually sessile (Figs. 7C, 7D, and 7E). In contrast, one couple was seen post cloacal as small and vestigial (Fig. 7D). The male body ends with a small papillary-like structure (Fig. 7E). The caudal appendix starts on its dorsal surface; however there is no pronounced striation.

Females of *P. ambiguus* have lateral wings in the anterior part of the body and plugs on the ventral surface. The tail was long, with noticeable loops, and it terminated with an exposed, pin-like tip (Figs. 8C and 8D). Prominent bands or annular structures (Figs. 8C and 8D) characterize the tail of mature females. As the worm approaches maturity, these bands increase in number and prominence, beginning at the posterior end of the large portion of the tail toward the anus. No bands could be detected in young or medium-sized specimens. The tail exhibits fine striations over the entire length, even showing through the annular bands.

B- Molecular analysis

Partial domains D1 and D2 of the 28S rDNA gene were amplified and sequenced for *Passalurus ambiguus* belonging to the families of Taeniidae Ludwig, 1886. The PCR amplification ranged from 700 to 800 bp. The sequence data of *Passalurus ambiguus* (781 nucleotides) examined were deposited in GenBank with accession numbers MZ571165.

The obtained sequences were aligned with 12 reference sequences representing the Oxyuroidea available species (Table 3); three species of *Thelandros* (*T. galloti*, *T. tinerfensis*, and *T. filiformis*); two species of *Pharyngodon* (*P. micipsae* and *P. echinatus*) and *Skrijabinema* (*S. ovis* and *S.*

longicaudatum); one species of *Batracholandros* (*B. salamandrae*), *Passalurus* (*P. ambiguus*), *Oxyuris* (*O. equis*), *Heteroxynema* (*H. cucullatum*), and *Aspicularis* (*A. tetraptera*) together with *Ascaridia galli* (Ascaridiidae) as an outgroup. Thus, all sequences (including outgroup) were aligned over 872 positions.

The phylogenetic analysis was done using ML and MP methods. The obtained phylogenetic trees are shown in Figs. 9 and 10.

Phylogenetic trees based on the partial 28S sequence data showed that the superfamily Oxyuroidea was divided into four monophyletic clades, representing three families. Family Pharyngodonidae included genera of *Pharyngodon* (*P. micipsae* and *P. echinatus*), *Thelandros* (*T. galloti*, *T. tinerfensis*, and *T. filiformis*) and *Batracholandros* (*B. salamandrae*). Family Oxyuridae included genera of *Passalurus* (*P. ambiguus*), *Oxyuris* (*O. equis*), and *Skrjabinema* (*S. ovis* and *S. longicaudatum*), and were divided into two monophyletic clades. Family Heteroxynematidae included *Heteroxynema* (*H. cucullatum*) and *Aspicularis* (*A. tetraptera*).

In the phylogenetic tree constructed by the ML method, representatives of the family Oxyuridae are distributed into two monophyletic clades. Clade 1 included *Passalurus ambiguus*, representing the subfamily Syphaciinae. Clade 2 included *Oxyurisequis*, *Skrjabinema ovis*, and *S. longicaudatum*, representing the subfamily Oxyurinae.

In the phylogenetic tree constructed by the MP method, *Oxyurisequis* separated from members of *Skrjabinema*, and it acts as a basal clade to the rest of included members of Oxyuroidea.

The present *Passalurus ambiguus* clustered together with the same species that having accession no. KY990018 with a strong bootstrap value (ML = 100, MP = 100). *Skrjabinema ovis* clustered together with *Skrjabinema longicaudatum* in a strong bootstrap value (ML = 100, MP = 100).

The genetic distance, estimated from 28S partial sequences, between the present *Passalurus ambiguus* and the previously recorded *P. ambiguus* was small (1.2%). The value between the *Pharyngodonmicipsae*, *P. echinatus*, and *Thelandrogalloti* was small (1.7%). In contrast, high values between *Thelandrogalloti* and *T. tinerfensis* and *T. filiformis* were observed (10.6% to 10.8%), as shown in Table 3. Therefore, the genetic distances support is consistent with the constructed phylogenetic trees (Figs. 9 and 10).

C- Pathological findings

The macroscopic appearance of the appendix was enlarged and filled with white nodules (Fig. 1A). The worms also appeared in the rectum pellets and were separated (Figs. 1B, C)

The histopathological examination revealed numerous nematode worms (*Passalurus ambiguus*) infested the appendiceal layers, particularly inside the germinal layer of the lymphoid follicle and appendiceal lumen (Figs. 11, 12). The worm detection mainly inside crypts deeply into the follicles, causing hyperplasia in the lymphoid tissues and the follicular epithelium cells (Fig. 13). The transverse section of *Passalurus ambiguus* with the anterior and posterior portions contained eggs, displayed beneath the hyperplastic cells, where lymphocyte and eosinophil cells aggregated and surrounded it (Fig. 14). Granulomatous reaction was induced due to cells injury and aggregation of chronic inflammatory cells against the worm infestation, with inflammatory edema surrounded it (Fig. 15). Appendicitis manifested with a heavy worm infestation accumulated inside the lumen, leading to hyperplasia in the epithelial lining of crypts and follicles projected to form papillary formation causing narrowing and obstruction with worm and cell debris, besides hypertrophy of their follicles with reactive lymphocytes (Figs. 16 A, B).

Discussion

Oxyurids are nematode parasites that are found all over the world and have serious public health consequences (Abdel-Gaber, 2016; Khalil et al., 2014). *Passalurus* species (Oxyuridae) have been found in domestic and wild rabbits, but only a few research have concentrated on these nematodes (Millazzo et al., 2010; Robles and Navone, 2007; Sotillo et al., 2012). *Passalurus ambiguus* Rudolphi, 1819, *P. nonanulatus* Skinker, 1931, *P. abditus* Caballero, 1937, *P. parvus* Johnston and Mawson, 1938, and *P. assimitis* Wu, 1933 are the five species in this genus. *Passalurus ambiguus* is an ambiguous species of *Passalurus*, and it was originally described in the Palearctic region among *Oryctolagus cuniculus* and *Lepus europeus* Hall, 1916. *Passalurus ambiguus* is the most frequent intestinal worm found in Egyptian rabbits. The present species share morphological features with *Passalurus*, including the triangular mouth opening provided by four papillae and three teeth; the shape and size of the spicule; the lack of the gubernaculum and the location of the male cloacal papillae (Dos Santos et al., 2017; Hugot et al., 1983; Petter and Quentin, 2009; Sultan et al., 2015; Vicente et al., 1997; Yamaguti, 1961). Based on the mentioned factors, the current species has been identified as *P. ambiguus*. The current species were morphologically and morphometrically compared to that obtained by Abdel-Gaber et al. (2019) and Rodriguez et al. (1974), and it was found to be strikingly similar to *P. ambiguus*. The investigation by Abdel-Gaber et al. (2019) and Rodriguez et al. (1974) revealed similar results, with only minor changes in body part measurements.

Bin and Chunsheng (1987) mentioned the presence of lips in *P. ambiguus* in a brief comment, despite the fact that practically all known keys (Hugot et al., 1983; Vicente et al., 1997; Petter and Quentin, 2009) and the current study do not reference such a structure. It is possible that they mistook the head papillae, or the three teeth-like features, for lips, which led to the erroneous reference to such a morphological characteristic.

In males, SEM gave a clear view of the cloacal region topography. There are three papillae pairs (the first two pairs were pericloacal and larger than the last pair, which was small, sessile, and barely postcloacally located.). This finding is consistent with the description of a male *P. ambiguus* given by Hugot et al. (1983), Sultan et al. (2015) and Abdel-Gaber et al. (2019). Furthermore, another pair of small papillae has been observed, located in the region where the tail narrows and the caudal appendage begins, which is also a feature of male *P. ambiguus* described by Skinker (1931). It is well known that the number and position of papillae in the cloacal region are estimated differently between species. Skinker (1931) and Hugot et al. (1983) confirmed this variation based on the nature of the insemination process in *Passalurus*; researchers later used these features to distinguish *P. ambiguus* from other described species of *Passalurus*.

The tail topography of females distinguished *P. ambiguus* from *P. nonanulatus*, as the latter lacks the distinctive transverse cuticular striations that give *P. ambiguus* its moniliform appearance. Light microscopy can detect this unique appearance, but the SEM best observes it in accordance with those given by Sultan et al. (2015) and Abdel-Gaber et al. (2019). Based on the criteria provided, the results show that the female samples collected here are those of *P. ambiguus*.

There are three families of Oxyuroidea (Chabaud, 1974). The Pharyngodonidae includes parasites mainly found in the posterior gut of herbivorous lower vertebrates, with a few species parasitizing mammals (Petter and Quentin, 1976). The Oxyuridae and the Heteroxynematidae contain many species infesting mammals and only a few species infesting birds; these parasites are notably widespread in the caeca of lizards, terrestrial tortoises, marsupials, rodents, and primates.

The Oxyuridae are classified into three subfamilies, including Oxyurinae, Enterobiinae, and Syphaciinae, with tribes in the subfamily Syphaciinae (i.e., Syphaciini, Acanthoxyurini, Higertiini, Passalurini, and Protozoophagini). The monophyly of Oxyurinae and Syphaciinae was confirmed by the current phylogenetic analyses. The findings support the previous hypotheses (Hugot, 1988; Adamson, 1989; Hugot et al., 1996; Li et al., 2019; Cao et al., 2020). The current study is the first to use phylogenetic analyses based on 28S sequence data to determine the systematic position of *Passalurus ambiguus* among Egyptian domestic rabbits. The *Passalurus ambiguus* clade was found to be monophyletic. This result was similar to Li et al. (2019) and Cao et al. (2020). *Oxyuris equis* formed a monophyletic group with *Skrjabinema ovis* and *S. longicaudatum*, consistent with the findings of Li et al. (2019) and Cao et al. (2020).

Mejia-Madrid (2018) observed that *Skrjabinema ovis* clustered with *Passalurus ambiguus*, and *Oxyuris equis* was a sister species to them in a monophyletic group with a significant support value (BI = 100). This may be explained due to insufficient data in the GeneBank for members of *Passalurus* and *Skrjabinema*.

The data set showed that *Thelandros* was paraphyletic, in which *T. galloti* was inserted within the *Parapharyngodon* clade. De Sousa et al. (2019) obtained this finding, but they reported that *Thelandros* seemed to be polyphyletic. According to Astasio-Arbiza et al. (1988), *T. galloti* shares some morphological characters associated with *Parapharyngodon* (i.e., caudal alae are absent and lateral alae are long and wide). *Thelandros galloti*, *Parapharyngodon micipsae*, and *P. echinatus* were recorded from lacertids in Spain.

Our study revealed chronic inflammation due to worm irritation (*Passalurus ambiguus*) on the appendix layers, causing hyperplasia and hypertrophy in epithelial cells and lymphoid follicles with lumen obstruction. Some studies support the findings of acute or chronic inflammation in pinworm-infested appendix specimens. However, most studies show that appendiceal pinworms cause fewer inflammatory changes (Panidis et al., 2011). Few studies have looked into the histopathology of *Passalurus ambiguus* in domestic rabbits (Mykhailiutenko et al., 2019). To our knowledge, this study is the first focusing on the presence of *P. ambiguus* in the appendix of domestic rabbits with histopathological examination. In conclusion, the current findings indicate that the pinworm species infecting Egyptian domestic rabbits is *P. ambiguus* Rudolphi, 1819.

Declarations

Acknowledgments

The authors would like to thank the Electron Microscopy Unit at South Valley University for their direct help and technical assistance with scanning electron microscopic investigations and EKB editing service for English editing of manuscript.

Author contribution

Nermean M. Hussein: investigation, methodology, writing—review and editing. Soheir A. H. Rabie: supervision, writing—review and editing. Wafaa A. Abuelwafa: collecting samples, methodology, writing—original draft. Mouchira M. Mohi Eldin: writing—review and editing the histopathological part.

Funding

Not applicable.

Data availability

The materials used during the current study are available by the authors.

Ethics approval

The National Ethics Committee of South Valley University and veterinary authorities in South Valley University Province, Egypt, approved the method of this study.

Consent to participate

Not applicable.

Consent for publication

Not applicable.

Conflict of interest

The authors declare no competing interests.

References

1. Abdel-Gaber R (2016) *Syphacia obvelata* (Nematode, Oxyuridae) infecting laboratory mice *Mus musculus* (Rodentia, Muridae): phylogeny and host–parasite relationship. *Parasitology Research* 115(3):975–985
2. Abdel-Gaber R, Ataya F, Fouad D, Daoud M, Alzuhairy S (2019) Prevalence, morphological and molecular phylogenetic analyses of the rabbit pinworm, *Passalurus ambiguus* Rudolphi 1819, in the domestic rabbits *Oryctolagus cuniculus*, *Acta Parasitologica* 64(2): 316–330
3. Adamson ML (1989) Evolutionary biology of the Oxyurida (Nematoda): biofacies of a haplodiploid taxon, *Advances in Parasitology* 28: 175–228
4. Astasio-Arbiza P, Zapatero-Ramos LM, Solera-Puertas MA, González-Santiago PM (1988) *Thelandros galloti* n. sp. (Nematoda, Pharyngodonidae) sobre *Gallotia galloti galloti* Duméril y Bibron, 1839, lacértido endémico de Tenerife (Islas Canarias), *Revista Ibérica de Parasitología* 48(3): 283–288
5. Bin Z, Chunsheng B (1987) Scanning electron microscopic observations of the integumental surface of adult *Passalurus ambiguus*, *Acta Zoologica Sinica* 33(4): 383–384
6. Cao YF, Chen HX, Li Y, Zhou DW, Chen SL, Li L (2020) Morphology, genetic characterization and molecular phylogeny of pinworm *Skrjabinema longicaudatum* n. sp. (Oxyurida: Oxyuridae) from the endangered Tibetan antelope *Pantholops hodgsonii* (Abel) (Artiodactyla: Bovidae), *Parasites and Vectors* 13(1):1
7. Chabaud AG (1974) Keys to subclasses, orders and superfamilies No. 1. In: Anderson, R.C., Chabaud, A.G., Willmott, S. (eds), *CIH keys to the nematode parasites of vertebrates*, (Commonwealth Agricultural Bureaux, Farnham Royal, UK): 1-17
8. Danheim BL, Ackert JE (1929) On the anatomy of the nematode *Passalurus ambiguus* (Rudolphi), *Transactions of the American Microscopical Society* 48(1): 80–85
9. De Belloq JG, Ferté H, Depaquit J, Justine JL, Tillier A, Durette-Desset MC (2001) Phylogeny of the Trichostrongylina (Nematoda) inferred from 28S rDNA sequences, *Molecular Phylogenetics and Evolution* 19(3): 430–442
10. De Sousa A, Jorge F, Carretero MA, Harris DJ, Roca V, Perera A (2019) The importance of integrative approaches in nematode taxonomy: the validity of *Parapharyngodon* and *Thelandros* as distinct genera, *Journal of Helminthology* 93(5): 616–628
11. Dos Santos FAA, Carvalho C, Nuno O, Correia JJ, Henriques M, Peleteiro MC, Fevereiro M, Duarte MD (2017) Detection of rabbit haemorrhagic disease virus 2 during the wild rabbit (*Oryctolagus cuniculus*) eradication from the Berlengas archipelago, Portugal, *BMC Veterinary Research* 13(1): 1
12. El-Akabawy LM, Zayan KA, Tantawy AA, Omar REM (2004) Anticoccidial efficacy of propolis and toltrazuril against *Eimeria stiedae* in New Zealand White Rabbit's, *Zagazig Veterinary Journal* 32(1): 129–145
13. Georgi JR, Georgi ME (1990) *Parasitology for veterinarians*, Saunders, Philadelphia.
14. Grice RL, Prociw P (1993) In vitro embryonation of *Syphacia obvelata* eggs, *International Journal for Parasitology* 23(2): 257–260
15. Hugot JP (1988) Les nématodes Syphaciinae, parasites de rongeurs et de lagomorphes. *Mémoires du Muséum National d'Histoire Naturelle* 141: 13–149
16. Hugot JP, Bain O, Cassone J (1983) Sur le genre *Passalurus* (Oxyuridae: Nematoda) parasite de leporidés, *Systematic Parasitology* 5(4): 305–316

17. Hugot JP, Gardner SL, Morand S (1996) The Enterobiinae subfam. Nov. (Nematoda, Oxyurida) pinworm parasites of primates and rodents, *International Journal for Parasitology* 26(2): 147–159
18. Khalil AI, Lashein GH, Morsy GH, Abd El-Mottaleb DI (2014) Oxyurids of wild and laboratory rodents from Egypt, *Life Science Journal* 11(3): 94–107
19. Li H, Shao R, Song N, Song F, Jiang P, Li, Z, Cai W (2015) Higher-level phylogeny of paraneopteran insects inferred from mitochondrial genome sequences. *Scientific Reports* 5(1): 8527
20. Li Y, Chen HX, Yang XL, Li L (2019) Morphological and genetic characterization of *Syphabulea tjanschani* (Ablasov, 1962) (Nematoda: Oxyuridae), with phylogenetic position of *Syphabulea* in Oxyuridae. *Infection, Genetics and Evolution* 67: 159–166
21. Mejia-Madrid HH (2018) A molecular phylogeny of the Rhigonematomorpha De Ley & Blaxter, 2002 as inferred from SSU and LSU rDNA sequences, *Nematology* 20(6): 547–565
22. Meyer MC, Olsen OW (1975) *Essentials of parasitology*. 2nd ed., (Brown Company, Wm. C., Publishers)
23. Milazzo C, Ribas A, Casanova JC, Cagnin M, Geraci F, Bella C (2010) Helminths of the brown rat (*Rattus norvegicus*) (Berkenhout, 1769) in the city of Palermo, Italy, *Helminthologia* 47(4): 238–240.
24. Mykhailiutenko SM, Kruchynenko OV, Klymenko OS, Serdioucov JK, Dmytrenko NI, Tkachenko VV (2019) Pathomorphological changes in the large intestine of rabbits parasitised by *Passalurus ambiguus* (Nematoda, Oxyuridae), *Regulatory Mechanisms in Biosystems* 10(1): 69-74
25. Ogedengbe ME, El-Sherry S, Whale J, Barta JR (2014) Complete mitochondrial genome sequences from five *Eimeria* species (Apicomplexa; coccidia; Eimeriidae) infecting domestic turkeys, *Parasites and Vectors* 7(1): 335
26. Owen D (1972) *Common parasites of laboratory rodents and lagomorphs*, (Laboratory animals centre handbook no. 1. Medical Research Council)
27. Panidis S, Paramythiotis D, Panagiotou D, Batsis G, Salonikidis S, Kaloutsis V, Michalopoulos A (2011) Acute appendicitis secondary to *Enterobius vermicularis* infection in a middle-aged man: a case report, *Journal of Medical Case Reports* 5(1): 559
28. Petter AJ, Quentin JC (1976) Keys to genera of the Oxyuroidea-No. 4. In: Anderson RC, Chabaud AG, Willmott S (eds), *CIH keys to the nematode parasites of vertebrates*. Commonwealth Agricultural Bureaux, Farnham Royal UK, pp: 1-30
29. Petter AJ, Quentin JC (2009) Oxyuroidea. In: Anderson, R.C., Chabaud, A.G., Willmott, S. (eds), *Keys to the nematode parasites of vertebrates (Archival Volume)*, (CAB International, London) 218–247
30. Rosario Robles R MR, Navone GT (2007) A new species of *Syphacia* (Nematoda: Oxyuridae) from *Oligoryzomys nigripes* (Rodentia: Cricetidae) in Argentina, *Parasitology Research* 101(4): 1069–1075
31. Rodriguez RJ, Pozo GD, Herrera LJ (1974) Estudios sobre el genero *Passalurus* Dujardin, 1845, parasitando al *Oryctolagus cuniculus domesticus* (L.) y *Lepus granatensis* R, *Revista Iberica de Parasitologia* 33: 315–329
32. Sheng L, Cui P, Fang SF, Lin, RQ, Zou, FC, Zhu XQ (2015) Sequence variability in four mitochondrial genes among rabbit pinworm (*Passalurus ambiguus*) isolates from different localities in China, *Mitochondrial DNA* 26(4): 501–504
33. Skinker MS (1931) Three new parasitic nematode worms. *Proceedings of the United States National Museum* 79(2890) 1–9
34. Solórzano-García B, Falcón-Ordaz J, Parra-Olea G, Pérez-Ponce de León G (2020) *Batracholandros salamandrae* (Oxyuroidea: Pharyngodonidae) in endemic salamanders (Amphibia: Plethodontidae) of the trans-Mexican volcanic belt: host range wide distribution or cryptic species complex? *The Journal of Parasitology* 106(5): 633–643
35. Sotillo J, Trelis M, Cortés A, Luz Valero M, del Pino MS, Esteban JG, Marcilla A, Toledo R (2012) Proteomic analysis of the pinworm *Syphacia muris* (Nematoda: Oxyuridae), a parasite of laboratory rats, *Parasitology Research* 61(4): 561–564
36. Sultan K, Elhawary NM, Sorour SSG, Sharaf HM (2015) Observations of the rabbit pinworm *Passalurus ambiguus* (Rudolphi, 1819) in domestic rabbits (*Oryctolagus cuniculus*) in Egypt using a scanning electron microscope, *Tropical Biomedicine*, 32(4): 745–752
37. Taffs LF (1976) Pinworm infections in laboratory rodents: a review, *Laboratory Animals* 10(1): 1-13
38. Vicente JJ, Rodrigues HO, Gomes DC, Pinto RM (1997) Nematóides do brasil. Parte V: Nematóides de mamíferos, *Revista Brasileira de Zoologia* 14(1): 1–14
39. Yamaguti S (1961) *Systema Helminthum: Volume I. The nematodes of vertebrates. Part I and II* (Interscience Publisher, New York)
40. Yang D, Ren Y, Fu Y, Xie Y, Nie H, Nong X, Gu X, Wang S, Peng X, Yang G (2013) Genetic variation of *Taenia pisiformis* collected from Sichuan, China, based on the mitochondrial cytochrome B gene, *The Korean Journal of Parasitology* 51(4): 449–452

Tables

Table (1): Estimation of evolutionary divergence between the present sequences of *Passalurus ambiguus* and the previously recorded sequences of Oxyuroidea.

| | 1 | 2 | 3 | 4 | 5 | 6 | 7 | 8 | 9 | 10 | 11 | 12 | 13 |
|---|-------|-------|-------|-------|-------|-------|-------|-------|-------|-------|-------|-------|-------|
| *MZ571165 <i>Passalurus ambiguus</i> | | | | | | | | | | | | | |
| KY990018 <i>Passalurus ambiguus</i> | 0.012 | | | | | | | | | | | | |
| MH459244 <i>Parapharyngodon micipsae</i> | 0.224 | 0.213 | | | | | | | | | | | |
| MH459237 <i>Parapharyngodon echinatus</i> | 0.221 | 0.210 | 0.005 | | | | | | | | | | |
| MT341271 <i>Batracholandros salamandrae</i> | 0.231 | 0.212 | 0.086 | 0.086 | | | | | | | | | |
| MH459230 <i>Thelandros galloti</i> | 0.217 | 0.204 | 0.017 | 0.018 | 0.091 | | | | | | | | |
| MH459216 <i>Thelandros tinerfensis</i> | 0.218 | 0.200 | 0.103 | 0.099 | 0.113 | 0.106 | | | | | | | |
| MH459218 <i>Thelandros filiformis</i> | 0.216 | 0.195 | 0.111 | 0.107 | 0.111 | 0.108 | 0.026 | | | | | | |
| MH011017 <i>Heteroxynema cucullatum</i> | 0.251 | 0.237 | 0.154 | 0.156 | 0.152 | 0.149 | 0.150 | 0.147 | | | | | |
| MH215351 <i>Aspiculuris tetraptera</i> | 0.255 | 0.242 | 0.156 | 0.152 | 0.155 | 0.153 | 0.150 | 0.147 | 0.101 | | | | |
| KY990021 <i>Oxyuris equi</i> | 0.272 | 0.264 | 0.198 | 0.195 | 0.204 | 0.193 | 0.170 | 0.181 | 0.183 | 0.196 | | | |
| KY990019 <i>Skrjabinema ovis</i> | 0.258 | 0.241 | 0.187 | 0.184 | 0.177 | 0.184 | 0.175 | 0.178 | 0.196 | 0.209 | 0.212 | | |
| MW020100 <i>Skrjabinema longicaudatum</i> | 0.263 | 0.247 | 0.199 | 0.193 | 0.193 | 0.197 | 0.181 | 0.183 | 0.194 | 0.217 | 0.224 | 0.086 | |
| KY990014 <i>Ascaridia galli</i> | 0.332 | 0.315 | 0.246 | 0.244 | 0.248 | 0.244 | 0.217 | 0.223 | 0.251 | 0.262 | 0.273 | 0.269 | 0.278 |

Table (2): Comparative measurements (mm) of *Passalurus ambiguus* Rudolphi (1819) with those previously described.

| Reference | Rodriguez et al. (1974) | Abdel-Gaber et al. (2019) | Present study |
|------------------|------------------------------|------------------------------|------------------------------|
| Host | <i>Oryctolagus cuniculus</i> | <i>Oryctolagus cuniculus</i> | <i>Oryctolagus cuniculus</i> |
| Locality | Tunisia | Cairo, Egypt | Qena, Egypt |
| Male | | | |
| Body length | 4.500 | 4.400 (3.600–5.700) | 4.622 (2.838 - 7.172) |
| Body width | 0.150 | 0.150 (1.200 - 0.170) | 2.788 (1.394 - 5.583) |
| Esophagus | | | |
| Total length | 0.560 | 0.580 (0.520 - 0.640) | 0.710 (0.391- 1.238) |
| Corpus length | — | 0.340 (0.290 – 0.370) | 0.538 (0.274 - 0.908) |
| Diameter of bulb | 0.150 | 0.14 (0.13–0.16) | 0.165 (0.094 - 0.304) |
| Spicule length | 0.125 | 0.110 (0.090 - 0.180) | 0.094 (0.068 -0.153) |
| Tail length | 0.500 | 0.530 (0.460 – 0.620) | 0.298 (0.145- 0.492) |
| Female | | | |
| Body length | 8.200 | 1.130 (9.600–1.280) | 5.622 (2.347 – 9.532) |
| Body width | 0.550 | 0.630 (0.500–0.700) | 0.314 (0.185- 0.381) |
| Esophagus | | | |
| Total length | 0.600 | 0.620 (0.570–0.680) | 0.484 (0.435- 0.571) |
| Corpus length | — | 0.420 (0.340–0.490) | 0.369 (0.325- 0.451) |
| Diameter of bulb | 0.130 | 0.180 (0.150–0.190) | 0.124 (0.100 – 0.146) |
| Tail length | 2.200 | 0.340 (0.200–0.380) | 0.828 (0.579- 0.945) |
| Egg length | 0.080–0.110 | 0.070 (0.060–0.096) | 0.080 (0.075- 0.088) |
| Egg width | 0.040–0.050 | 0.047 (0.035–0.058) | 0.034 (0.034- 0.035) |

Table (3): Partial 28S rDNA sequences of oxyuroidean species used in this study with their host species, locality and GenBank accession numbers. (*sequences collected from present study).

| Species | Host | Locality | Accession No. | Reference |
|------------------------------------|------------------------------|-------------------------|---------------|--------------------------------|
| <i>Passalurus ambiguus</i> | <i>Oryctolagus cuniculus</i> | USA | KY990018 | Mejia-Madrid , 2018 |
| <i>Passalurus ambiguus</i> | <i>Oryctolagus cuniculus</i> | Qena Governorate, Egypt | MZ571165 | Present study* |
| <i>Oxyuris equi</i> | --- | USA | KY990021 | Mejia-Madrid , 2018 |
| <i>Skrjabinema longicaudatum</i> | <i>Pantholops hodgsonii</i> | China | MW020100 | Cao et al., 2020 |
| <i>Skrjabinema ovis</i> | <i>Capra hircus</i> | USA | KY990019 | Mejia-Madrid , 2018 |
| <i>Parapharyngodon echinatus</i> | <i>Gallotia stehlini</i> | Spain | MH459237 | De Sousa et al. (2018) |
| <i>Parapharyngodon micipsae</i> | <i>Podarcis carbonelli</i> | Spain | MH459244 | De Sousa et al. (2018) |
| <i>Thelandros tinerfensis</i> | <i>Gallotia caesaris</i> | Spain | MH459216 | De Sousa et al. (2018) |
| <i>Thelandros filiformis</i> | <i>Gallotia galloti</i> | Spain | MH459218 | De Sousa et al. (2018) |
| <i>Thelandros galloti</i> | <i>Gallotia caesaris</i> | Spain | MH459230 | De Sousa et al. (2018) |
| <i>Heteroxynema cucullatum</i> | --- | --- | MH011017 | Bell et al. (2018) |
| <i>Batracholandros salamandrae</i> | <i>Pseudoeurycea leprosa</i> | Mexico | MT341271 | Solorzano-Garcia et al. (2020) |
| <i>Ascaridia galli</i> | <i>Gallus gallus</i> | USA | KY990014 | Mejia-Madrid , 2018 |

Figures

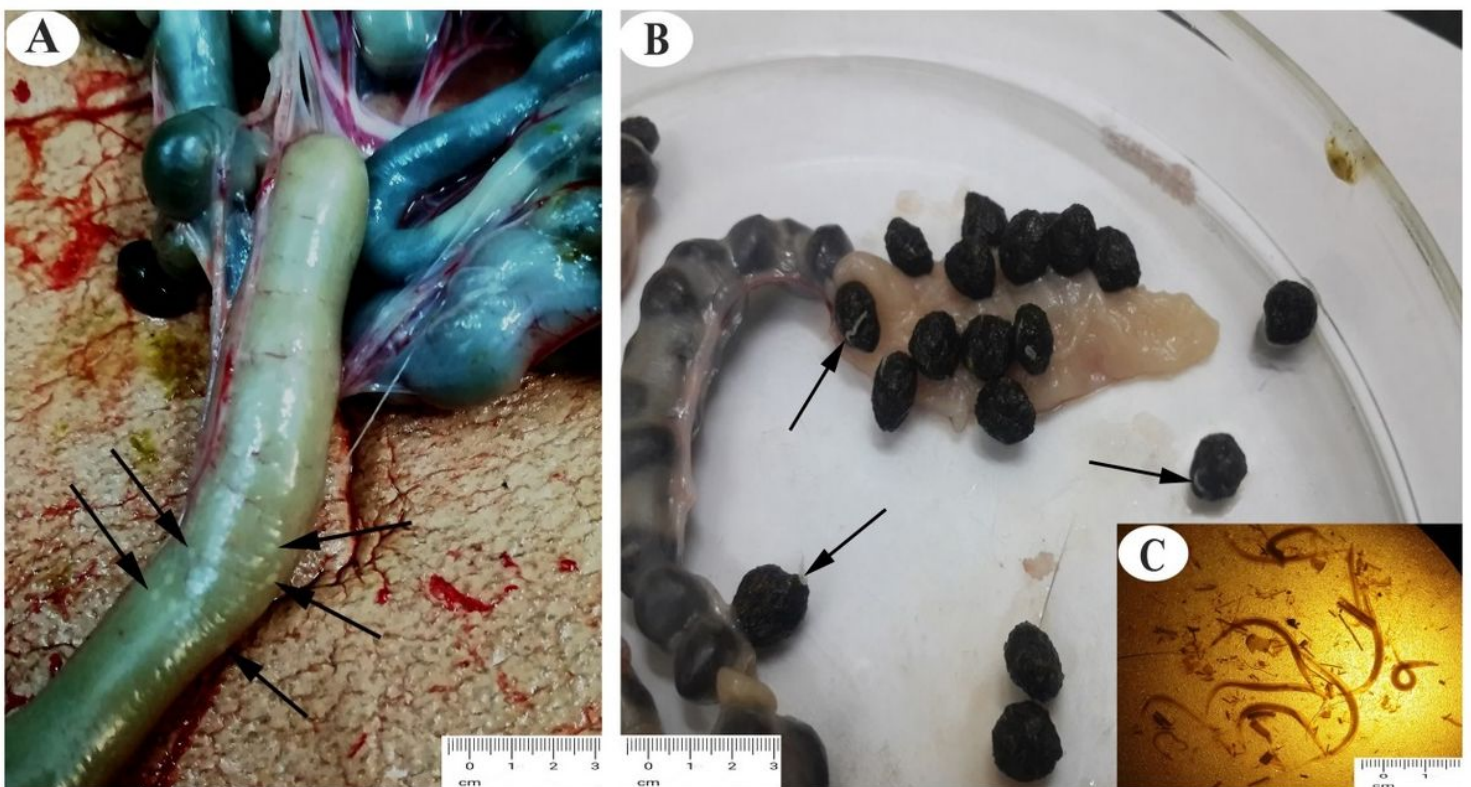


Figure 1

Photographs of *Passalurus ambiguus* in the appendix and rectum of domestic rabbits. (A): The enlarged appendix showing small white nodules. (B): Worms attached in fecal pellets. (C): Worms (males and females).

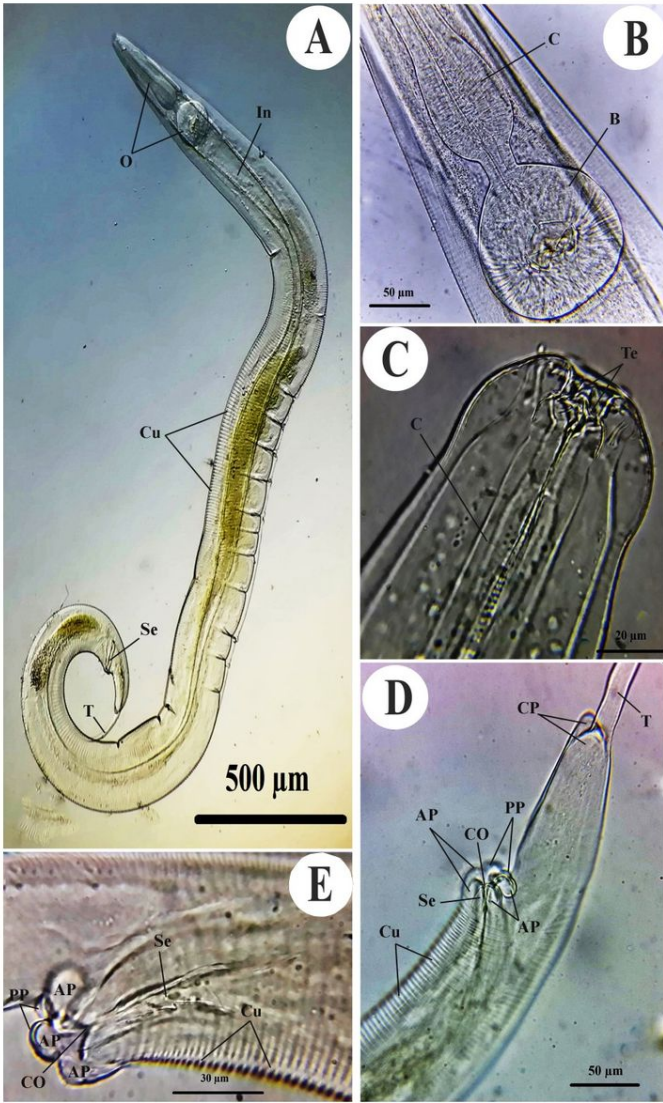


Figure 2

Light photomicrographs of the male of *Passalurus ambiguus* isolated from the large intestine of domestic rabbits in Qena Governorate, Upper Egypt, mounted in lactophenol. (A) Adult worm. (B & C) The anterior portion of the worm. (D & E) The posterior portion of the worm. Scale bars; A, 500 µm; B & D, 50 µm; C, 20 µm; E, 30 µm. Abbreviations; AP, anterior papillae; B, bulb; C, corpus; CO, cloacal opening; Cu, cuticle; CP, caudal papilla; In, intestine; O, esophagus; PP, posterior papillae; Se, spicule; St, striations; T, tail; Te, teeth.

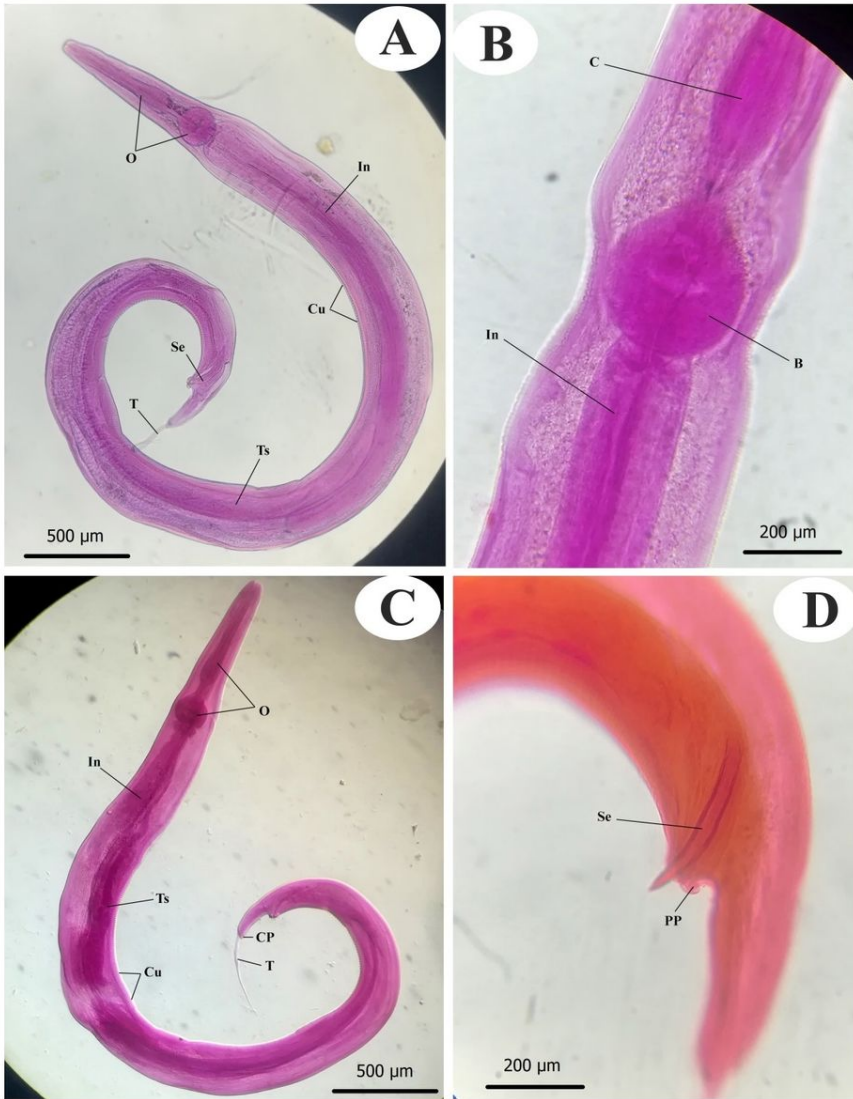


Figure 3

Light photomicrographs of the male of *Passalurus ambiguus* isolated from the large intestine of domestic rabbits in Qena Governorate, Upper Egypt stained with alum carmine. (A & C) Adult worms. (B) The anterior portion of the worm. (D) The posterior portion of the worm. Scale bars; A & C, 500 µm; B & D, 200 µm. Abbreviations; B, bulb; C, corpus; Cu, cuticle; CP, caudal papilla; In, intestine; O, esophagus; PP, posterior papillae; Se, spicule; Ts, testis.

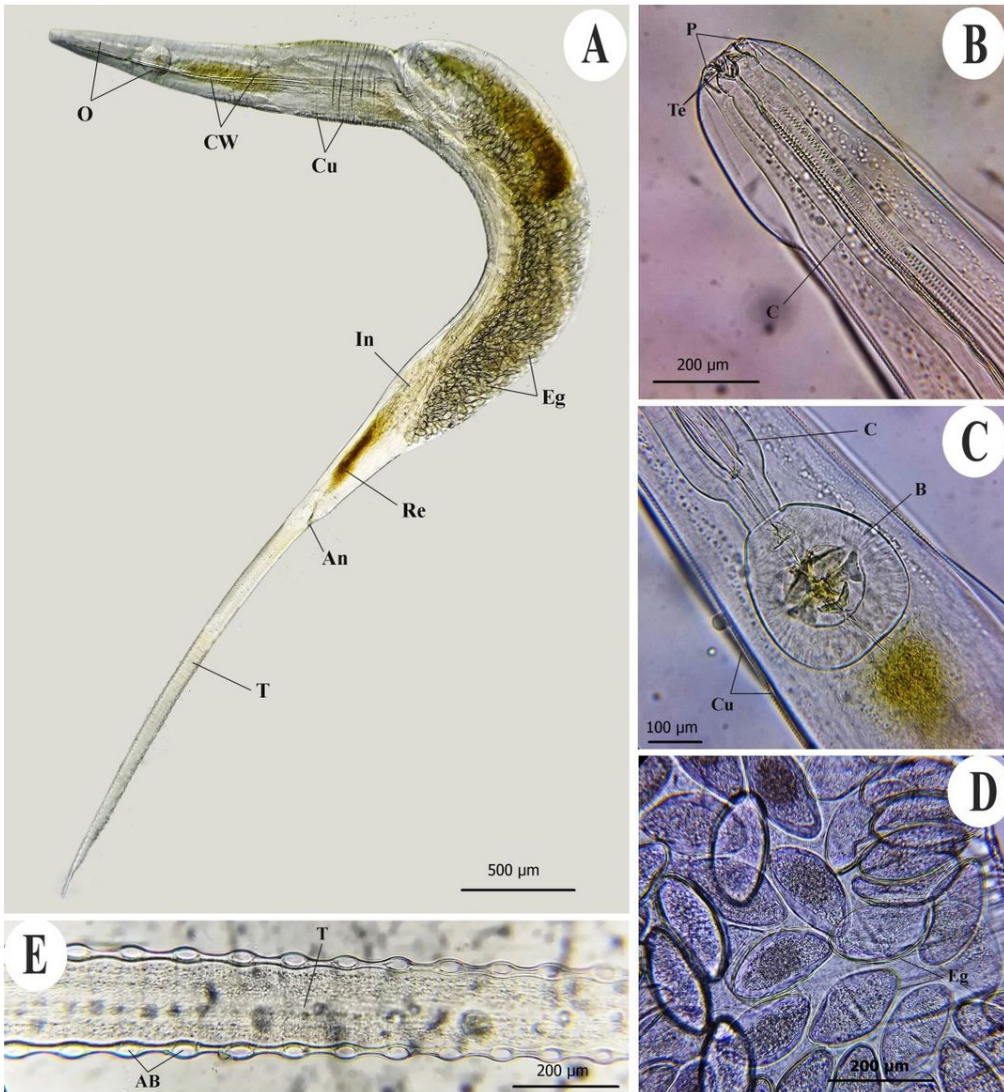


Figure 4

Light photomicrographs of the female *Passalurus ambiguus* isolated from the large intestine of domestic rabbits in Qena Governorate, Upper Egypt, mounted in lactophenol. (A) Adult worm. (B & C) The anterior portion of the worm. (D) Eggs. (E) The portion of the tail. Scale bars; A, 500 µm; B, D & E, 200 µm; C, 100 µm. Abbreviations; A, anus; AB, annular bands; B, bulb; C, corpus; Cu, cuticle; CW, cuticular wings; Eg, eggs; In, intestine; O, esophagus; P, papillae; Re, rectum; T, tail; Te, teeth

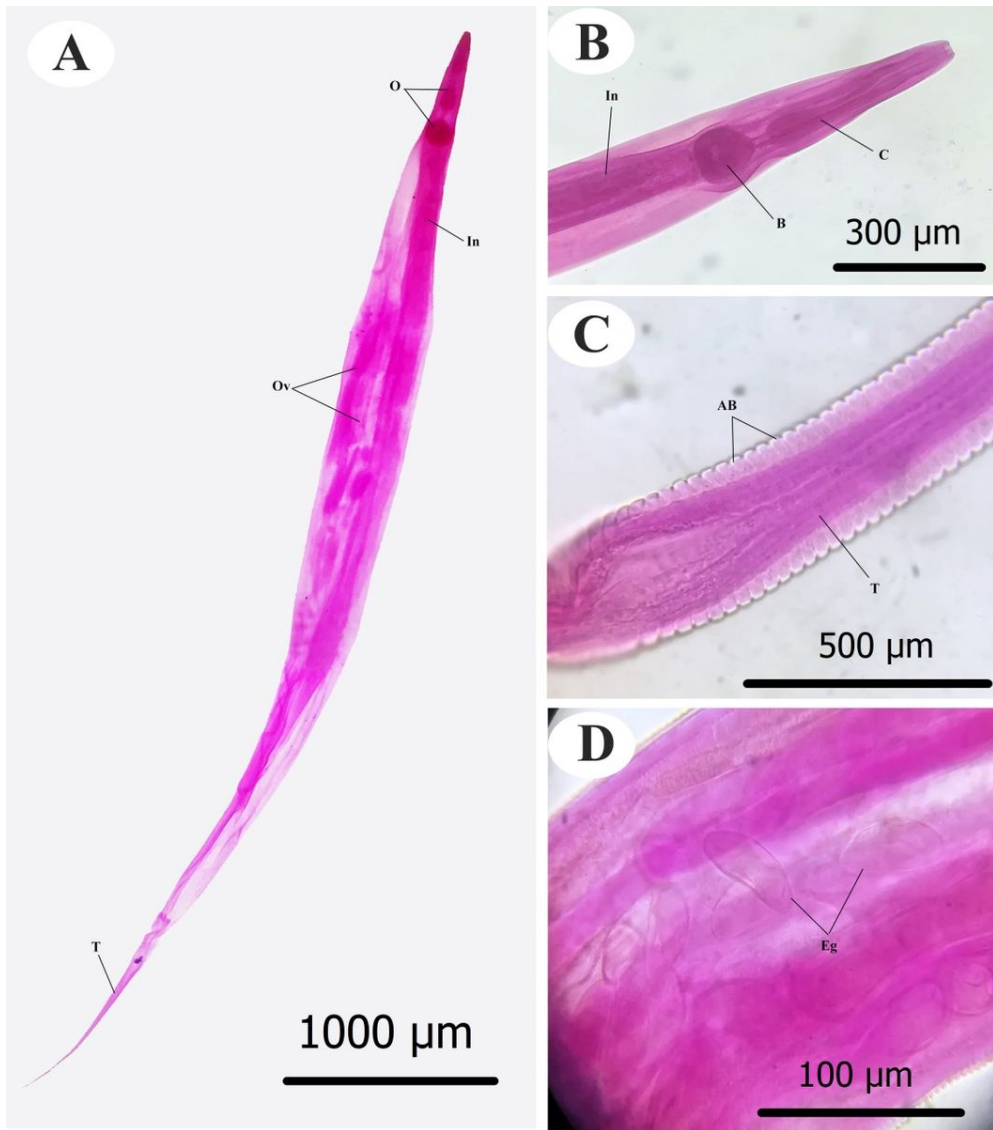


Figure 5

Light photomicrographs of the female *Passalurus ambiguus* isolated from the large intestine of domestic rabbits in Qena Governorate, Upper Egypt, stained with alum carmine. Fig. (A) Adult worm. Fig. (B) The anterior portion of the worm. Fig. (C) The portion of the tail. Fig. (D) Eggs. Fig. (E) The tail of the female. Scale bars; A, 1000 μm ; B, 300 μm ; C, 500 μm ; D, 100 μm . Abbreviations; AB, annular bands; B, bulb; C, corpus; Eg, eggs; In, intestine; Ov, ovaries; T, tail.

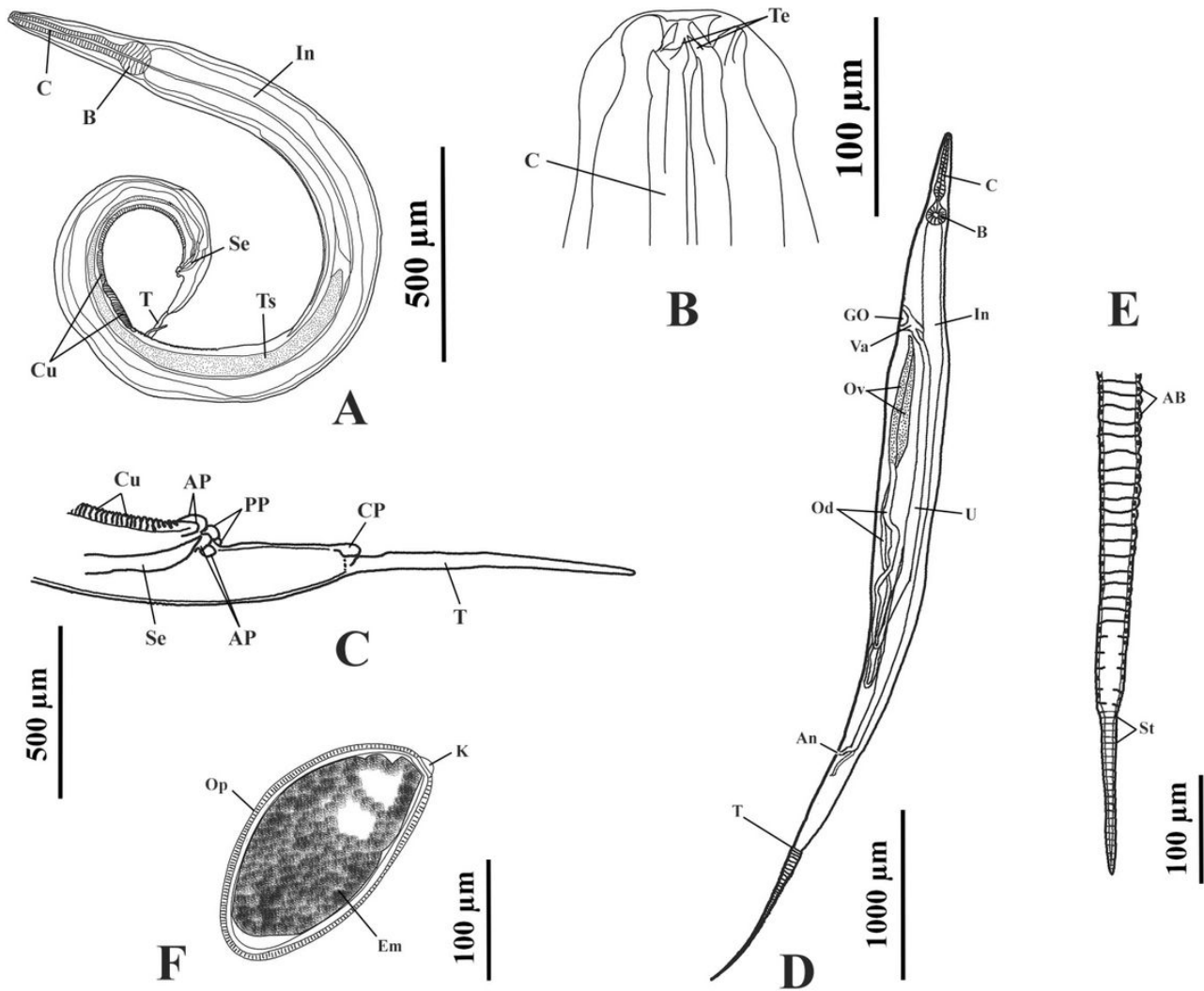


Figure 6

Line drawings of *Passalurus ambiguus* isolated from the large intestine of domestic rabbits in Qena Governorate, Upper Egypt. Fig. (A) Male of *Passalurus ambiguus*. Fig. (B) The anterior portion of the worm. Fig. (C) The posterior portion of the male. Fig. (D) Female of *Passalurus ambiguus*. Fig. (E) The tail of the female. Fig. (F) The egg. Scale bars; A & C, 500 μm ; B, D, E & F, 100 μm . Abbreviations; A, anus; AB, annular bands; AP, anterior papillae; B, bulb; C, corpus; Cu, cuticle; CP, caudal papilla; Em, embryo; GO, genital opening; In, intestine; K, knob; Od, oviducts; Op, operculum; Ov, ovaries; PP, posterior papillae; Se, spicule; St, striations; T, tail; Te, teeth; Ts, testis; U, uterus; Va, vagina.

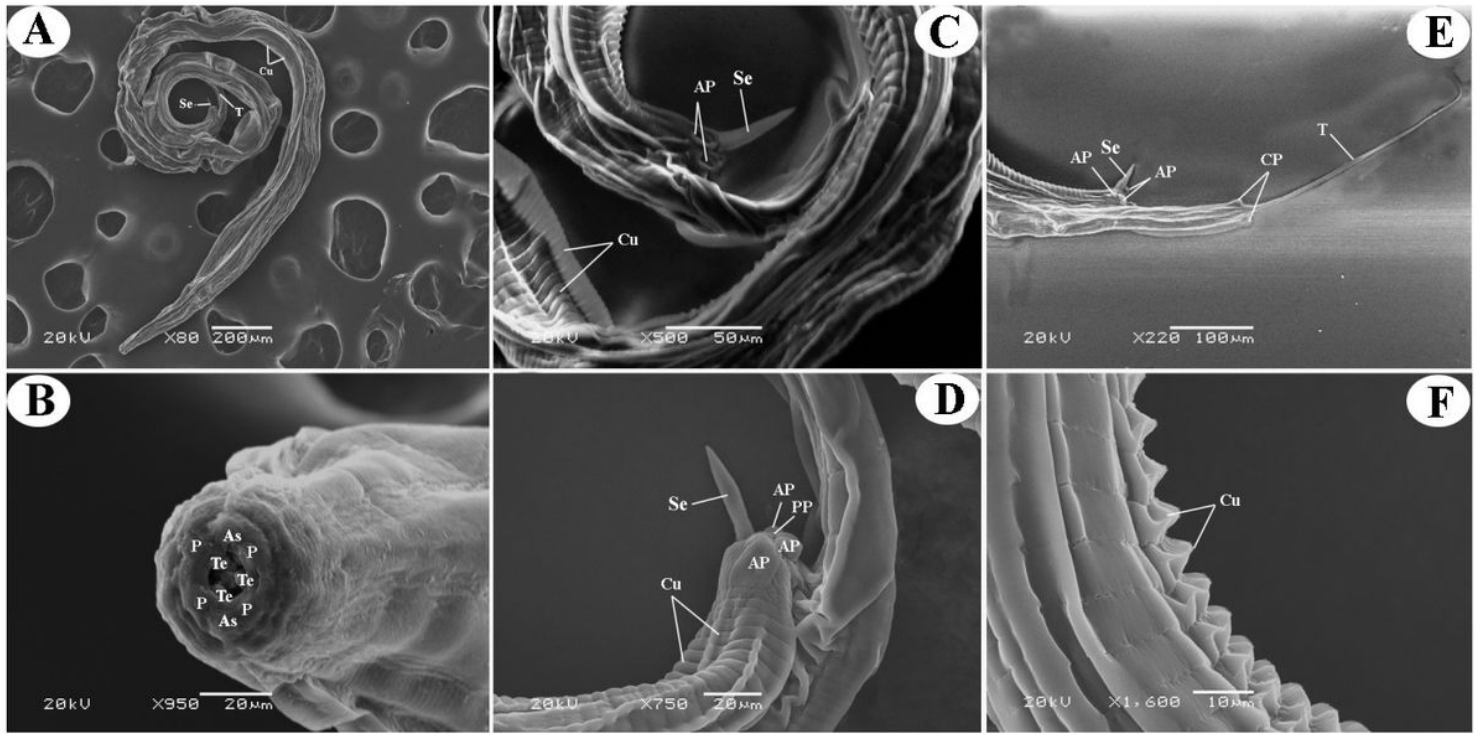


Figure 7

Scanning electron micrographs of the male of *Passalurus ambiguus* isolated from the large intestine of domestic rabbits in Qena Governorate, Upper Egypt. Fig. (A) Adult worm. Fig. (B) The anterior portion of the worm. Figs. (C, D & E) The posterior portion of the worm. Fig. (F) The cuticle. Scale bars; A, 200 μ m; B & D, 20 μ m; C, 50 μ m; E, 100 μ m; & F, 10 μ m. Abbreviations; As, amphids; AP, anterior papillae; Cu, cuticle; CP, caudal papilla; P, papillae; PP, posterior papillae; Se, spicule; T, tail; Te, teeth.

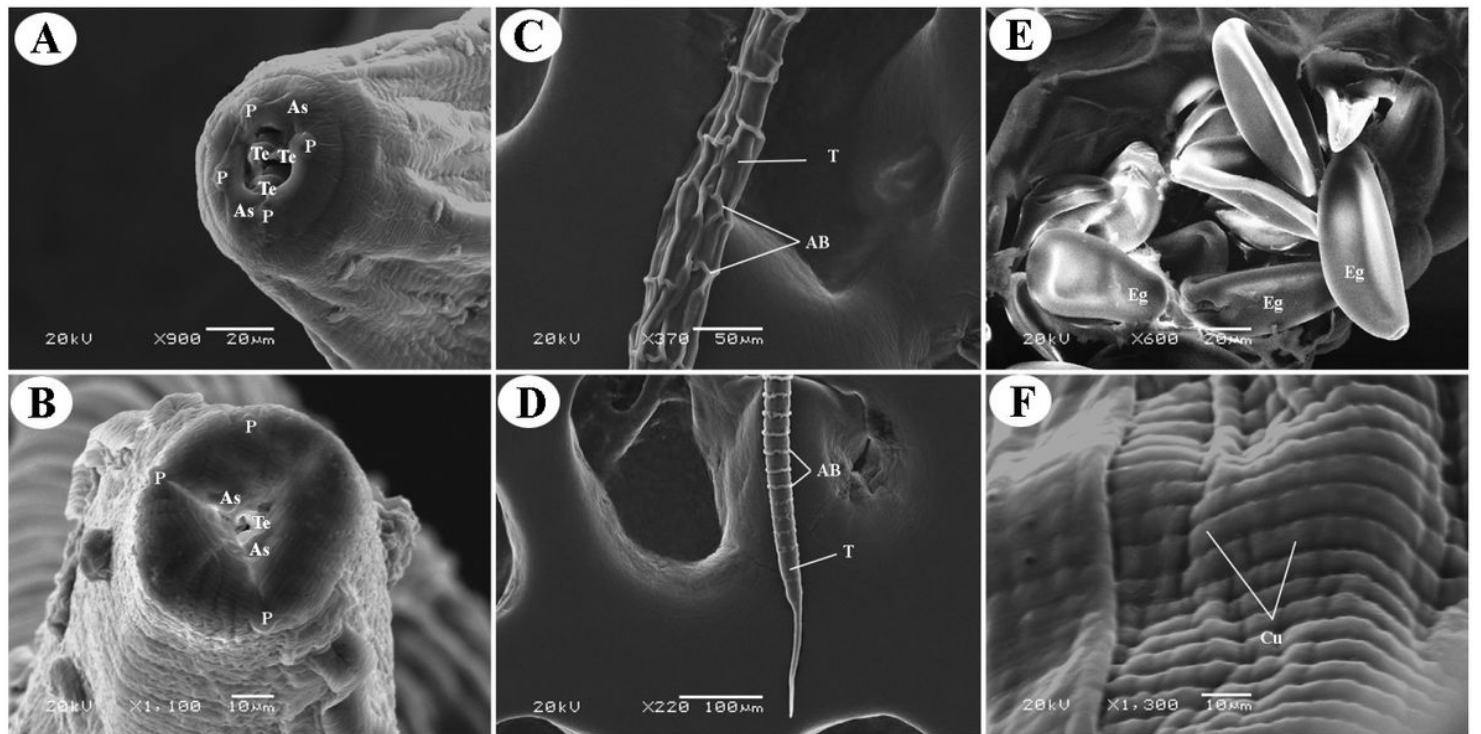


Figure 8

Scanning electron micrographs of the female of *Passalurus ambiguus* isolated from the large intestine of domestic rabbits in Qena Governorate, Upper Egypt. Figs. (A & B) The anterior portion of the adult worm. Fig. (C & D) The tail. Fig. (E) The eggs. Fig. (F) The cuticle. Scale bars; A & E, 20 μ m; B & F, 10 μ m; C, 50 μ m; D, 100 μ m. Abbreviations; As, amphids; AB, annular bands; Cu, cuticle; Eg, eggs; P, papillae; T, tail; Te, teeth.

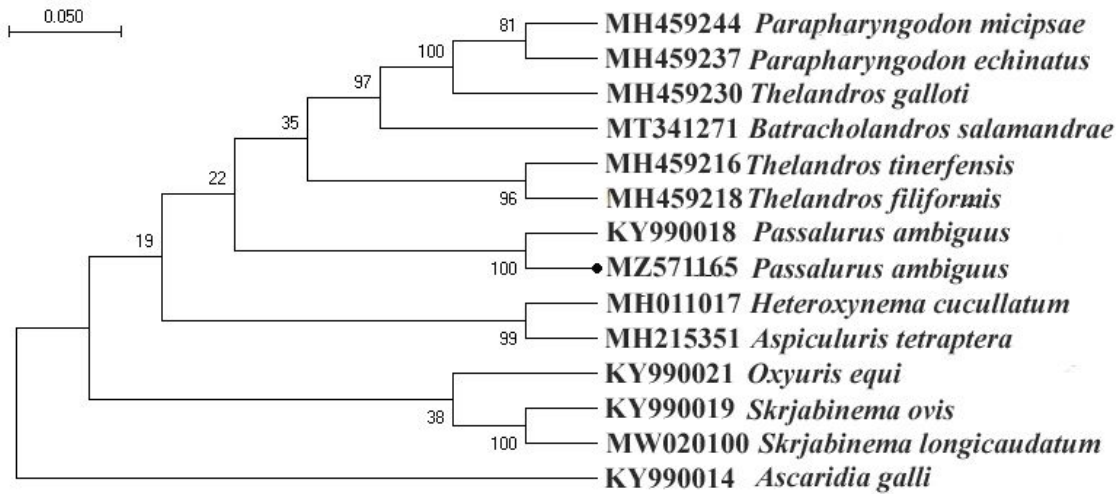


Figure 9

Maximum Likelihood (ML) tree based on the 28S sequence data showing the phylogenetic relationships of representatives of Oxyuroidea. *Ascaridia galli* belonging to the family Ascaridiidae was selected as an outgroup. The percentage of replicate trees in which the associated taxa clustered together in the bootstrap test (1000 replicates) is shown next to the branches.

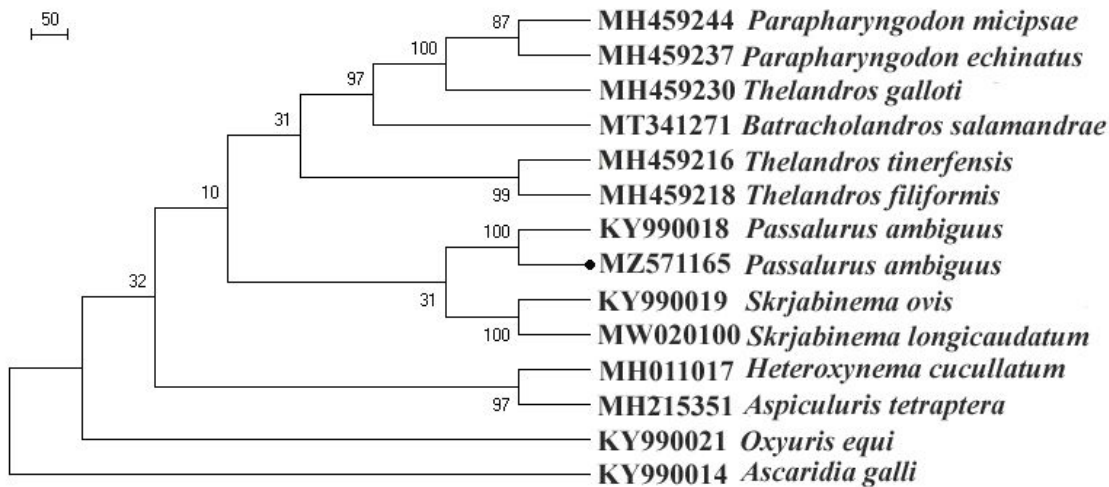


Figure 10

Maximum Parsimony (ML) tree based on the 28S sequence data showing the phylogenetic relationships of representatives of Oxyuroidea. *Ascaridia galli* belonging to the family Ascaridiidae was selected as an outgroup. The percentage of replicate trees in which the associated taxa clustered together in the bootstrap test (1000 replicates) is shown next to the branches.

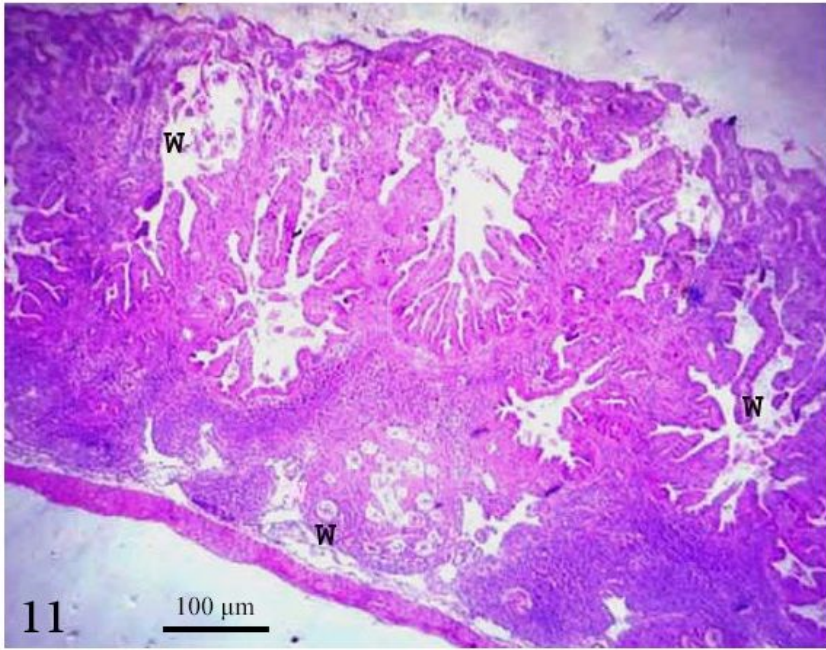


Figure 11

The appendix of rabbits infested with numerous nematode worm (W) (*Passalurus ambiguus*) in the appendiceal layers. (H&E., x4).

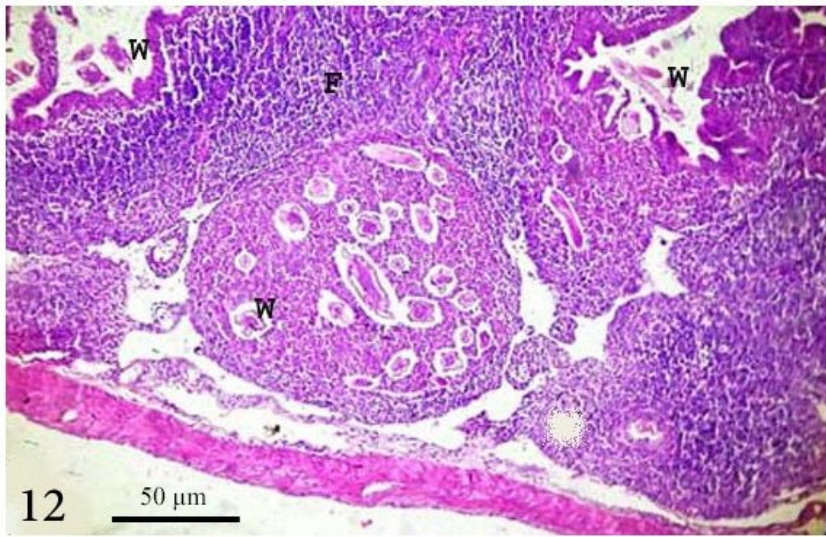


Figure 12

High power of the previous figure (Fig.11) to show the cross-section of the *Passalurus ambiguus* (W) inside the germinal layer of the lymphoid follicle (F) and appendiceal lumen(H&E., x10).

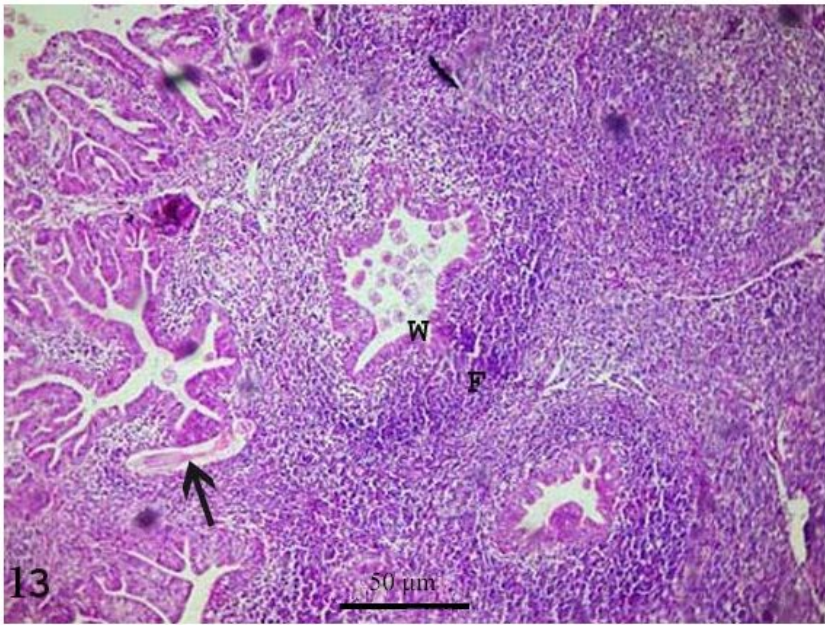


Figure 13

Appendix of rabbit showing the cross-section of worm (W) inside crypts deeply into hypertrophied follicles, other transverse section of worm (arrow) attached to hyperplastic epithelium cells. (H&E., x10).

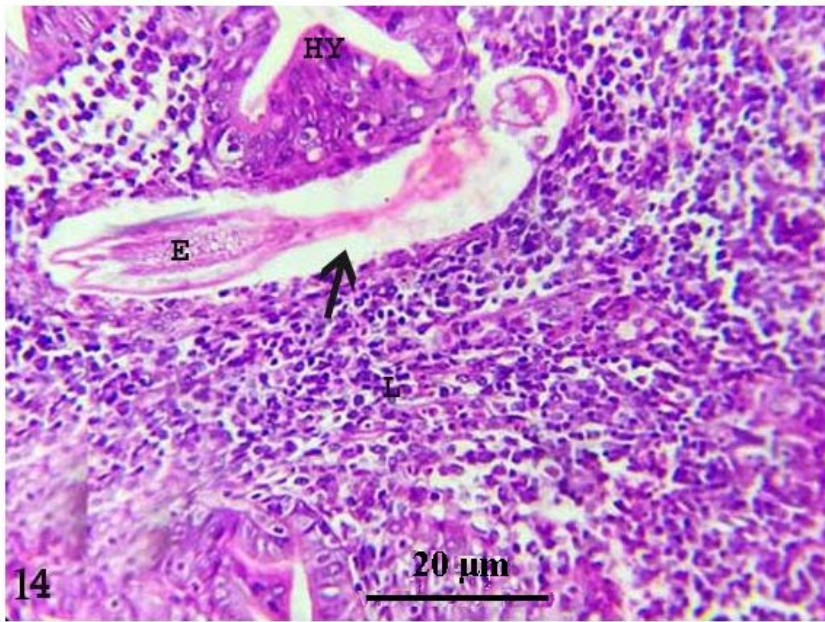


Figure 14

High power of the previous lesion (Fig. 13) to show the transverse section of *Passalurus ambiguus* (arrow) characterized with anterior and posterior portion containing egg inside its body, and surrounded with severely lymphocytes aggregation and eosinophils in addition to, hyperplasia in the epithelium lining (HY) of the crypts was noticed. (H&E., x40).

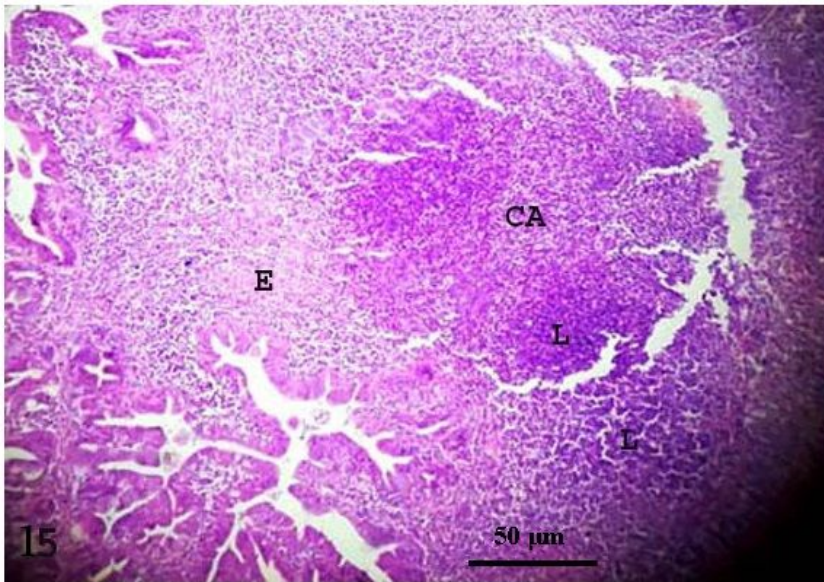


Figure 15

Appendix of rabbit showing granulomatous nodule (CA) appeared with the caseated area and severe aggregation of lymphocytes (L) in hypertrophied follicles and edema (E). (H&E., x10).

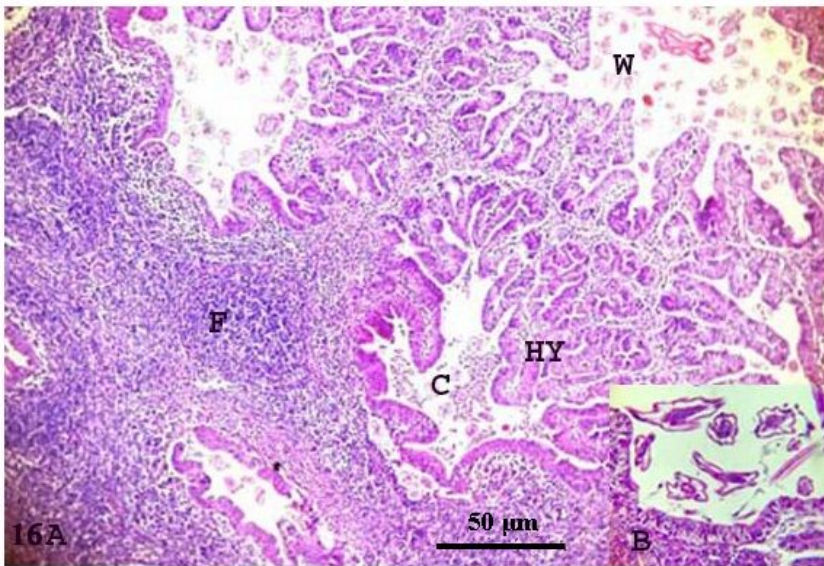


Figure 16

Appendix of rabbit showing (A) appendicitis manifested with a heavy infestation of worm (W) accumulated inside the lumen, leading to (HY) hyperplasia in the epithelial lining of crypts and follicles and obstruction with worm and cell debris (C), besides (F) hypertrophy of follicles with reactive lymphocytes. (B) High power to show the sections of the worm inside the lumen of the appendix. (H&E., x10).